

N73-28352

Paper M 13

**REMOTE SENSING OF OCEAN CURRENTS USING ERTS IMAGERY**

George A. Maul, *National Oceanic and Atmospheric Administration, Atlantic Oceanographic and Meteorological Laboratories, Miami, Florida*

**ABSTRACT**

Major ocean currents such as the Loop Current in the eastern Gulf of Mexico have surface manifestations which can be exploited for remote sensing. A time series to study certain aspects of the surface expression of this current was begun in August 1972. Surface chlorophyll-a concentrations, which contribute to the shift in color from blue to green in the open sea, were found to have high spatial variability; significantly lower concentrations were observed in the current. The cyclonic edge of the current is an accumulation zone which causes a peak in chlorophyll concentration. The dynamics also cause surface concentrations of algae, which have a high reflectance in the near infrared. Combining these observations gives rise to an "edge effect" which can show up as a bright lineation on multispectral imagery delimiting the current's boundary under certain environmental conditions. Frequently the sea-state in the current is higher than in surrounding water due to differential shear. When high seas introduce bubbles, white caps, and foam, the reflectance is dominated by scattering rather than absorption. This has been detected in ERTS imagery and used for current location.

1365

Original photography may be purchased from:  
EROS Data Center  
10th and Dakota Avenue  
Sioux Falls, SD 57198

PRECEDING PAGE BLANK NOT FILMED

## INTRODUCTION

The major circulation feature of the Gulf of Mexico is the so-called Loop Current. This flow enters the basin as a well formed western-boundary current through the Yucatan Straits. It penetrates into the Gulf to a varying latitude before it exits through the Straits of Florida. Transporting vast amounts of heat, salt and momentum, the current significantly affects circulation on the shelf, local fisheries, marine transportation, and is thought to be associated with hurricane intensification.

The current boundary separates two water masses. Across the boundary there is a difference in temperature, salinity, color, velocity, and biomass. These surface manifestations can be used for remote sensing in our efforts to monitor the current's variability. However, surface temperature difference, one of the best indicators, is not usable in the subtropics due to summer insolation which makes the sea surface isothermal. Other surface features, such as ocean color and evidences of horizontal current shear, probably have less seasonal variability.

This paper is a preliminary report on a time series of observations across the surface boundary layer of the Loop Current, and its detection by remote sensing, using several aspects of the surface features. The research is designed to investigate the seasonal variability of the juxtaposed water masses, both temporally and spatially, and the detection by ERTS of their boundary.

## FIELD EXPERIMENTS

The field work began in June 1972 with a ship/aircraft experiment designed to detect the color boundary of the Loop Current front south of Dry Tortugas. The NASA C-130 flew over the research vessel track which was oriented in the same azimuth as ERTS suborbital track. Seven altitudes were flown, at 100 mb decrements, over the ship. Aircraft data collection included RC-8 color and color IR photography as well as multispectral photography to simulate the ERTS MSS imagery, PRT-5 sea surface temperature profiles, Bendix 24 channel scanner data, and inflight recordings of atmospheric temperature, pressure and moisture.

Prior to the aircraft overflights the scientific crew aboard R/V BELLOWS located the boundary. Measurements of

ocean temperature, chlorophyll-a, volume scattering function, and salinity were made every ten meters down to 50 meters; Forel color, and upwelling and downwelling spectral irradiance were taken at each of the five stations that bracketed the front. During the overflights on the following day, closely spaced surface measurements of the same variables (except irradiance) were taken. All measurements were made using standard oceanographic techniques or analyzed by methods detailed by Strickland and Parsons (1968).

In August 1972 a time series of the Loop Current by ship and satellite was begun. The cruise plan is to occupy the suborbital track of ERTS that crosses the west Florida shelf approximately 200 kilometers west of Tampa and terminates in the center of the Yucatan Straits. Every 36 days, the R/V VIRGINIA KEY is on the suborbital track. Continuous surface observations of radiometric temperature (in conjunction with the NOAA-2 IR sensors) and chlorophyll-a (by the fluorometric method of Lorenzen, 1966) are made; at approximately 12 kilometer intervals XBT's are taken, and samples are drawn for salinity, bulk temperature, volume scattering function, and biomass analysis. At appropriate daylight stations, measurements of upwelling and downwelling spectral radiance are made using a 1/4 meter Ebert scanning spectro-radiometer. A standard hydrographic section of the Yucatan Straits is made in order to estimate the geostrophic transport relative to 800 db. After the section, the cyclonic edge of the current is tracked by following the pathline of the 22° C isotherm at 100 meters; this pathline loops from the western edge of Yucatan to the Florida Straits south of Dry Tortugas and is in close proximity to the surface front. Finally another hydrographic section is observed along the sub-orbital track of ERTS that passes from Key West to Havana.

It is planned to continue the cruises to collect one year of data in order to obtain an evaluation of the seasonal variability. The final field experiment, planned for the autumn, is a SKYLAB/EREP mission involving a ship and an aircraft.

#### PRELIMINARY RESULTS

The cyclonic edge of the Loop Current tends to concentrate flotsam and jetsam. Natural materials, such as surface marine algae, were seen from the June photo-

graphy to have a pinkish cast on color IR (SO 397) film; this is confirmed in black and white IR photography (type 2424 film and a 89B Wratten Filter). When these algae are present, they appear as a bright lineation marking the edge of the current in ERTS MSS-6 (0.7-0.8 $\mu$ m).

A second consequence of the boundary layer dynamics is to concentrate chlorophyll bearing organisms. A typical profile across the current boundary is given in figure 1. This transect is from Key West harbor, out the channel into the coastal water, and across the front. The feature of interest is the peak in chlorophyll-a concentration just at the boundary. This is a phenomenon noticed in each of the six cruises to date and occurs to a varying degree in the deep sea as well as near shore. Details of the variability will have to await further sampling because of expected seasonal and biological dependence. One would expect however that a shift towards the green would occur and enhance the boundary in MSS-4(0.5-0.6 $\mu$ m). This does indeed happen as will be discussed below.

A third observation is the usual change in sea state across the boundary. When winds and associated waves cross into zones of high current velocity with an opposing set, the seas generally build up rapidly. It is not uncommon for the sea state to increase from 1 to 2 meters when crossing into the current. Thus an increase of white caps, foam, and bubbles is encountered near the edge which increases the reflectance in the current. This raises the reflectance in all channels, but in a non-uniform (wavelength dependent) manner.

The term "edge effect" (Maul, 1972) was coined to describe these phenomena which can be exploited to detect the boundary of major ocean currents. Other streaming events, such as sediments being entrained by the Gulf Stream after passing source regions such as Cape Hatteras (ERTS 1132-15092), can be considered part of this edge effect. It allows a multispectral approach to recognize the boundary of these currents in the absence of sea surface temperature changes.

To understand the physics of reflection from the ocean, consider a simple model of an ocean of semi-infinite depth (Z) with spherical scattering. The spectral reflectance  $R(Z,-)$  is defined as the ratio of the

upwelling irradiance  $H(Z,+)$ , i.e. that from the ocean, to the downwelling irradiance  $H(Z,-)$ , i.e. that from the sky and sun:

$$R(Z,-) \equiv \frac{H(Z,+)}{H(Z,-)}$$

The reflectance is tacitly assumed to be a function of wavelength. From scattering theory the reflectance at the sea surface ( $Z=0$ ) can be shown to be

$$R(0,-) = 1 - H(\mu) \sqrt{1 - \omega_0}$$

where  $\omega_0$  is the ratio of the scattering coefficient ( $b$ ) to the attenuation coefficient ( $\alpha$ ),  $H(\mu)$  is the so-called H-function for various scattering albedos ( $\omega_0$ ) as tabulated by Chandrasekhar (1960) and  $\mu$  is the cosine of the zenith angle. It should be emphasized that this model does not include multiple scattering or the angular dependence of scattering such as the Monte Carlo calculations of Gordon and Brown (1973). Nevertheless it provides an analytic solution to the radiative transfer equation which illustrates the fundamental variables in reflectance.

An example of calculated reflectance from a plane water surface with the sun in the zenith [ $H(\mu_0)$ ] is given in figure 2. The curves are based on scattering and attenuation coefficients given by Jerlov (1968) for natural ocean water bodies;  $\alpha$  and  $b$  are chosen to exemplify the behavior of reflectance. Curve 1 is the spectral reflectance for pure water. Curve 2 is generated by changing the attenuation coefficient due to an increased absorption coefficient ( $a = \alpha - b$ ) due to yellow substance. Note that the reflectance is lower and that the peak has shifted to a longer wavelength. Curve 3 is generated by increasing the scattering coefficient due to isotropic scatters whose  $b$  is twenty times the Rayleigh (molecular) scattering at 450 nm.; only the magnitude of the scattering increases, in a wavelength dependent manner, with the peak invariant. Curve 4 combines the effects of absorption and scattering. The reflectance is lower than pure scattering and the wavelength of the peak is shifted to the green.

Curves 1 and 4 can be likened to the change in reflectance encountered when crossing an ocean front. An example of an observed reflectance pair is taken from

the June aircraft experiment and given in figure 3. These are uncorrected for the immersion effect and the reflectances are approximately 20% too high. The zenith angle was  $\sim 20^\circ$  in each case.  $H(Z,+)$  was measured 1 meter below the surface. The Loop Current water (marked 2) is lower in chlorophyll-a ( $< 0.1 \text{ mg m}^{-3}$ ) and lower in volume scattering coefficient ( $\beta(45)=2.6 \times 10^{-3} \text{ m}^{-1}$ ) than the coastal water (marked 4) with  $0.4 \text{ mg m}^{-3}$  chlorophyll-a and  $\beta(45)=5.4 \times 10^{-3} \text{ m}^{-1}$ . If one assumes that the absorption coefficient is proportional to the chlorophyll-a concentration and the scattering coefficient is proportional to the volume scattering coefficient at  $45^\circ$  (Beardsley *et al*, 1970) then a qualitative confirmation of reflectance theory is given.

The curves further suggest that changes in ocean color will be reflected in MSS-4. Figures 4a and b are images from ERTS-1 taken over the eastern Gulf of Mexico during times of surface observations. Figure 4a is MSS-4 data showing the higher reflectance of water from Florida Bay pouring over the Keys and being entrained by the Gulf Stream. This image confirms the discussion in the previous paragraph.

Figure 4b is MSS-5 data taken north of the Yucatan Straits during a period of surface observations. The curving discontinuity in the water masses outlines the edge of the current. However, the blue waters of the current are brighter than the adjoining waters in contradiction to the results in figure 3. The explanation must come from figure 2, where we see the effect of increased scatterers. A marked increase in sea state was encountered in the current, which can account for a much higher scattering coefficient due to entrapped air.

An additional explanation of this is offered through consideration of sea state alone. Ross and Cardone (1972) observed that with  $15 \text{ m s}^{-1}$  winds, 10% of the surface of the sea is covered with white caps, and white caps reflect approximately 90%. If reflectance of the ocean is assumed to be 5% in the absence of white caps and 10% of the sea is covered with white caps, then reflectance is  $R=5\%(.9) + 10\%(.9)=13.5\%$  or 270% higher than without white caps.

The spectrum of total upwelling irradiance from above the ocean  $H_T(0,+)= [R(0,-) + R_s]H(0,-)$  where  $R_s$  is the

reflectance of the surface (both diffuse and direct). For the case  $R_s = \text{constant}$  and a given  $H(0, -)$ ,  $H_T$  depends on  $\omega_0$ . From figure 2 we estimate that the ratio of  $R(0, -)$  at 450 nm to that at 525 nm for pure water is  $\sim 4.5$  (curve 1). The same ratio with scatterers only in the water (curve 3) is 2.0. Quantitative confirmation with realistic scattering phase functions will have to be calculated using the Monte Carlo code. Theoretically, the signal of a differential radiometer (Arvesen, 1972) is subject to such variation in  $\omega_0$ . If it is fortuitous that  $\omega_0$  always varies in the ocean such that  $R(0, -)_{\lambda_2}$  is constant (Duntley, 1972), then a dual channel instrument will work in the absence of sea state changes.

The solar spectrum is fairly flat in the visible region ( $H(0, -)_{450} / H(0, -)_{700} \sim 1.3$ ). Hence, higher sea states, which reflect high percentages of white light, proportionally add more long wavelength energy to the upwelling irradiance. In terms of a chromaticity diagram, this means that the purity changes but not the dominant wavelength. To correct for sea state a channel in a multispectral scanner near  $1 \mu\text{m}$  appears useful. At this wavelength there is a maximum in the attenuation coefficient of pure water (i.e.  $\omega_0 \rightarrow 0$ ), a maximum in atmospheric transmissivity, and the influence of chlorophyll seems low.

## CONCLUSIONS

ERTS imagery has been successful in providing information on the ocean in both the nearshore and deep sea environment. As the result of an edge effect the cyclonic side of the Gulf Stream can reflect in several ERTS bands as a prominent feature paralleling the current's edge. It is found however that sea state is a significant variable that can dominate the reflectance and change the spectral signature of surface waters. The prospect is therefore raised that passive remote sensing using ERTS may be used to quantitatively estimate sea state and near surface winds in areas of homogeneous water masses. Further, the sea state problem must be considered a dominant variable in the determination of ocean color from aerospace sensors.

## REFERENCES

- Arvesen, J. C. (1972). Fourth Annual Earth Resources Review, Vol. IV, NASA MSC-05937, pp. 104-1 to 104-2.
- Beardsley, G. F., H. Pak, K. Carder, and B. Lundgren (1970). Journal of Geophysical Research, 75 (15), pp. 2837-2845.
- Chandrasekhar, S. (1960). Radiative Transfer, Dover, New York, 393 pgs.
- Duntley, S. Q. (1972). Fourth Annual Earth Resources Review, Vol. IV, NASA MSC-05937, pp. 102-1 to 102-25.
- Gordon, H. R. and O. B. Brown (1973). Applied Optics. (in press).
- Jerlov, N. G. (1968). Optical Oceanography, Elsevier, New York, 194 pgs.
- Lorenzen, C. J. (1966). Deep Sea Research, 13, pp. 223-227.
- Maul, G. A., (1972). Interim Report on Remote Sensing of Ocean Currents from ERTS, NASA-CR-12907, National Technical Information Center, E72-10233.
- Ross, D. B. and V. Cardone (1972). Fourth Annual Earth Resources Review, Vol. IV, NASA MSC-05937, pp. 85-1 to 85-20.
- Strickland, J. D. H., and T. R. Parsons (1968). A Practical Handbook of Seawater Analysis. Fisheries Research Board of Canada, Ottawa, 311 pgs.



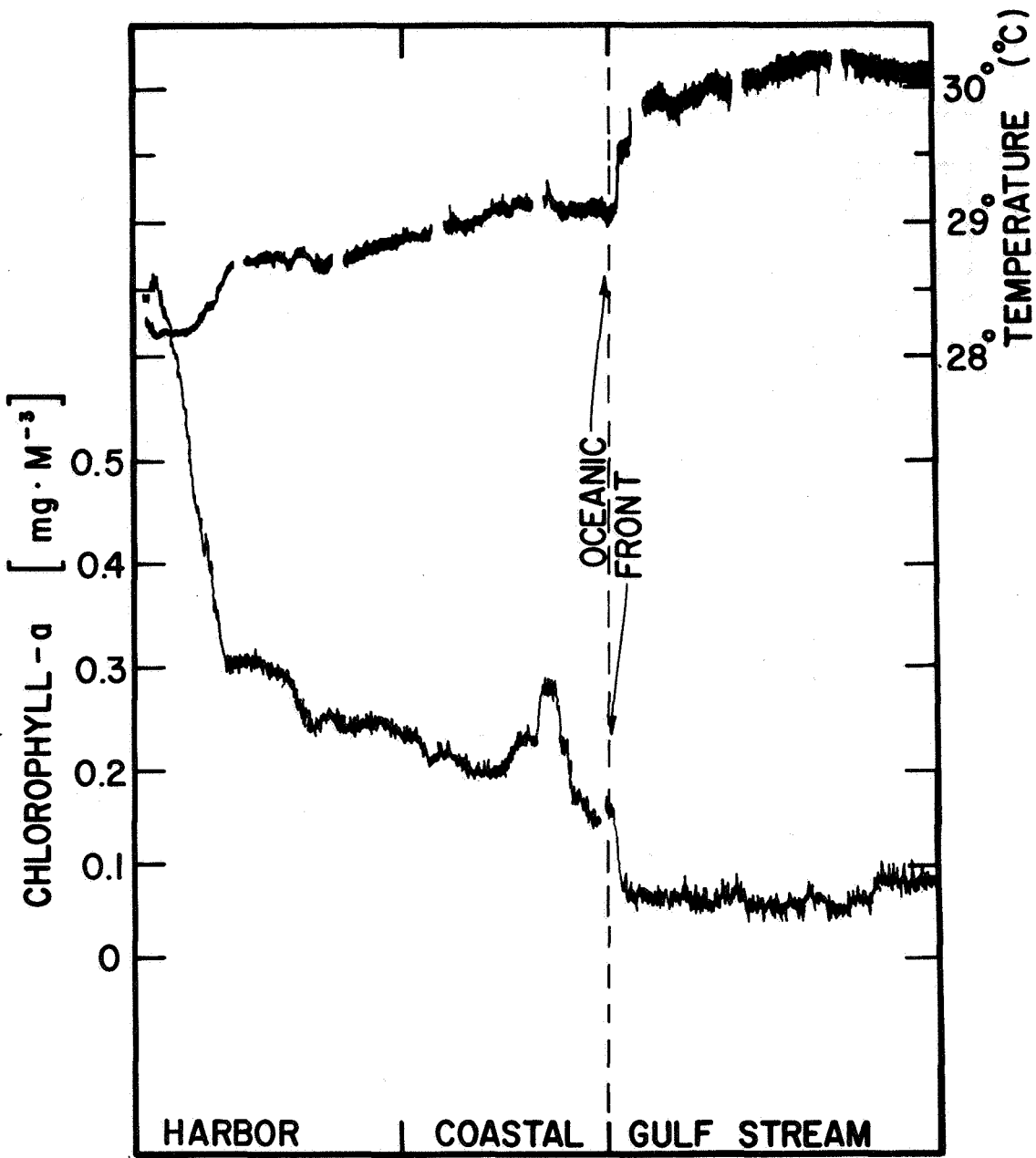


Figure 1: Surface temperature trace (upper) and surface chlorophyll-a profile (lower) across the Loop Current front and into Key West harbor. Horizontal scale across the figure is approximately 75 kilometers.

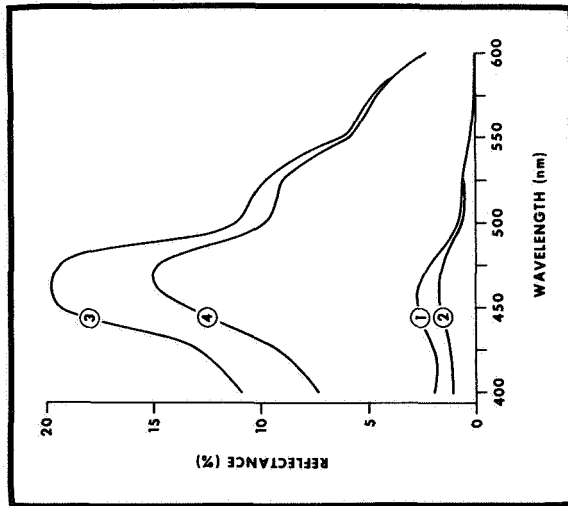


Figure 2: Results of theoretical calculations of reflectance from the water. 1 pure water, 2 pure water plus absorption due to yellow substance, 3 pure water plus isotropic scattering, 4 scattering plus absorption.

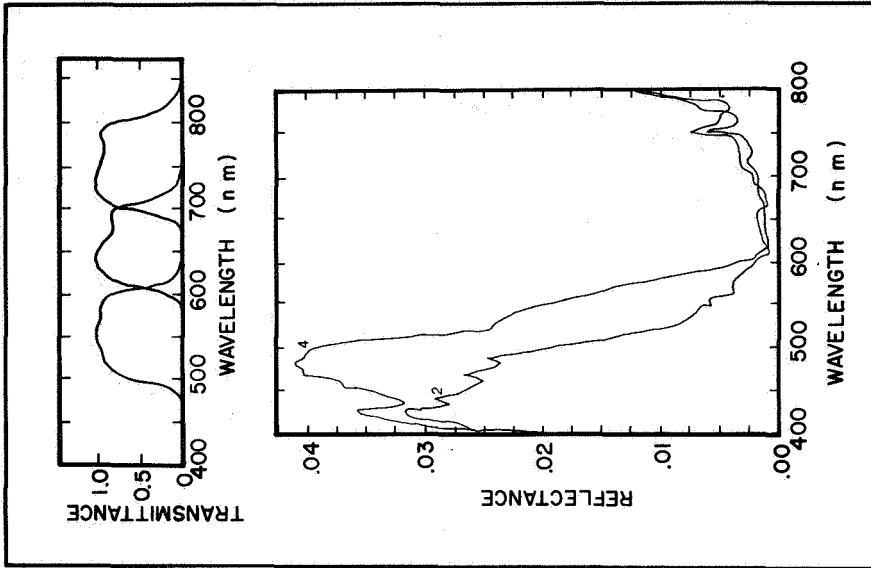


Figure 3: Observed reflectance across the Loop Current boundary. 2 current; 4 coastal water. Bottom depth exceeded 100 meters. Zenith angle about 15° in each case. The upwelling irradiance was measured at 1 meter depth. Upper panel has the spectral response of MSS 4, 5, and 6.

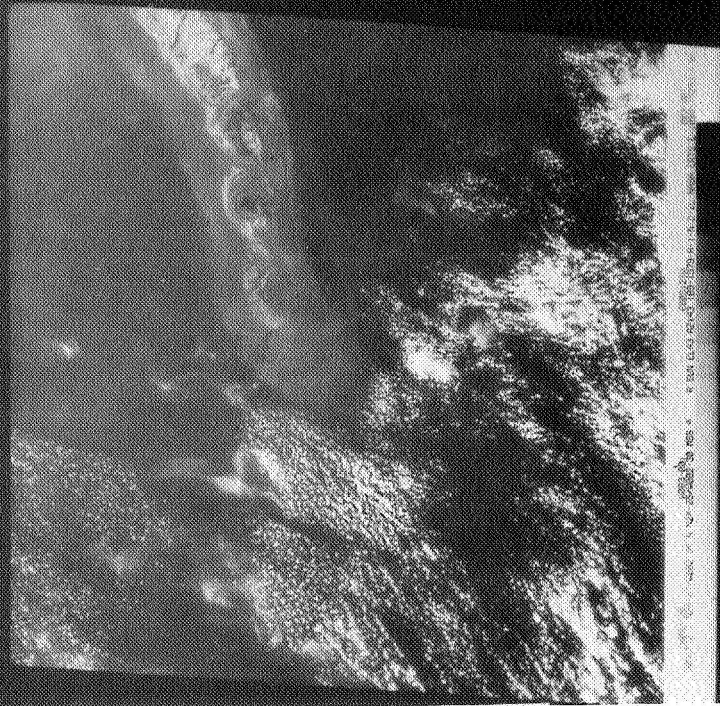


Figure 4a: MSS 4 imagery of the western Florida Keys showing water from Florida Bay being entrained by the Loop Current. The greener water from the bay appears brighter.



Figure 4b: MSS 5 imagery of the Loop Current exiting from the Yucatan Straits into the Gulf of Mexico. The blue water of the current appears brighter due to a higher sea state.